

ORIGINAL RESEARCH PAPER

## Exfoliated graphite/Selenium-Zinc Oxide Nanocomposites for Photodegradation of Organic Dye in Water and Its Antibacterial Activity Against Aater Borne Pathogens

Olubori Idowu Sonde <sup>1,2\*</sup>, Moses Gbenga Peleyeju <sup>2</sup>, Fatai Oladipupo Oladoyinbo <sup>1</sup>, Adejare Rasaq Oloyede <sup>4</sup>, Tajudeen Adeniyi Afolabi <sup>1</sup>, Hameed Adekola Adesokan <sup>1</sup>, Omotayo Ademola Arotiba <sup>2,3\*</sup>, Enoch Olugbenga Dare <sup>1</sup>

<sup>1</sup> Department of Chemistry, Federal University of Agriculture Abeokuta, Ogun State, Nigeria

<sup>2</sup> Department of Applied Chemistry, University of Johannesburg, Doornfontein 2028, South Africa

<sup>3</sup> Centre for Nanomaterials Science Research, University of Johannesburg, Doornfontein 2028, South Africa

<sup>4</sup> Biotechnology Centre, Federal University of Agriculture Abeokuta, Ogun State, Nigeria

Received: 2017-04-12

Accepted: 2017-05-22

Published: 2017-06-25

### ABSTRACT

We report the synthesis and application of a novel Exfoliated graphite/Selenium-Zinc oxide (EG/Se-ZnO) nanocomposite for photodegradation of methylene blue dye and its antibacterial activity. The composite was characterized using XRD, FTIR, SEM and TEM. Applicability of EG/Se-ZnO nanocomposite as photocatalyst was investigated by the photocatalytic degradation of methylene blue as a model for organic pollutant. The XRD has its highest peak at 101 which indicated that ion diffusion was free from solvent viscosity (peak at 002). FTIR spectra confirmed the formation of EG/Se-ZnO nanocomposite as band at 882 cm<sup>-1</sup> and 612 cm<sup>-1</sup>, 727 cm<sup>-1</sup>, 1373 cm<sup>-1</sup> were associated with vibrational frequency of ZnO lattice and Selenium respectively. The SEM revealed cloudy large particles of the synthesized EG/Se-ZnO composite. TEM image revealed mini-rodlike nanoparticles. 99.5% degradation of methylene blue dye was achieved within 90 minutes of irradiation. The reactions followed first order kinetics with the rate constant of 5.79x10<sup>-2</sup> min<sup>-1</sup> and R2 value of 0.9. The enhanced photocatalytic activity of EG/Se-ZnO was ascribed to the capability of graphitic layers to accept and transport electrons from the excited ZnO promoting charge separation. The antibacterial activity was also evaluated for the ZnO (bulk) and EG/Se-ZnO nanocomposite against the control (ciprofloxacin) and zone of inhibition observed was on E. coli and E. cloacae respectively depicted that EG/Se-ZnO was more effective on E. coli relatively to bulk ZnO. Thus, EG/Se-ZnO nanocomposite can be used for photocatalytic organic pollutant degradation.

**Keywords:** Nanocomposite, Photocatalyst, Photodegradation, Graphite, Selenium-Zinc oxide, Methylene blue  
© 2017 Published by Journal of NanoAnalysis.

### How to cite this article

Sonde OI, Peleyeju MG, Oladoyinbo FO, Oloyede AR, Afolabi TA, Adesokan HA, Arotiba OA, Dare EO. Exfoliated Graphite/Selenium-Zinc Oxide Nanocomposites for Photodegradation of Organic Dye in Water and Its Antibacterial Activity Against Water Borne Pathogens. J. Nanoanalysis., 2017; 4(1): 41-47. DOI: 10.22034/jna.2017.01.005

\* Corresponding Author Emails: [oarotiba@uj.ac.za](mailto:oarotiba@uj.ac.za), [sonde.idowu@gmail.com](mailto:sonde.idowu@gmail.com)

## INTRODUCTION

Wastewater disposal by industrial activities is the major concern to both environment and drinking water due to existence of several amounts of toxic materials. Such pollutants, their physical appearance seems to be the most obnoxious, as human eyes can easily recognize it. It is now a well-established fact that the coloration of water is mainly caused by dyes, which are generally toxic, non-decomposable and stable [3]. The stability of dyes towards light and oxidizing agents also create a problem for their removal by different waste treatment procedures. Therefore, their removal methods are selected with a great deal of care and consideration [2, 11, 8]. Before now, various technologies have been adopted for the removal of contaminants from industrial effluent includes, filtration, surface complexation, chemical precipitation, ion exchange, electrode position, membrane processing, flocculation etc. However, all these methods received some setbacks due to metal selectivity, low adsorption, and high consumption of chemicals and use of expensive equipment [10,15]. The photocatalytic decomposition of organic pollutants in wastewater received considerable research attention [6,10]. Amongst the photocatalysts studied for their photocatalytic properties,  $\text{TiO}_2$  is the most commonly used photocatalyst because of its high efficiency, low cost, nontoxicity and photochemical stability. Recently, another photocatalyst, ZnO, is receiving great attention from researchers [17, 18]. It was proved that ZnO displayed a similar photodegradation mechanism as  $\text{TiO}_2$  and was therefore proposed as a suitable alternative to  $\text{TiO}_2$  [17]. Several studies have highlighted that ZnO exhibits better efficiency than  $\text{TiO}_2$  for removing organic compounds in water bodies and photoelectric conversion. Studies have showed that ZnO nanoparticles can also be used as an antimicrobial agent [3]. The use of renewable and biodegradable materials such as  $\text{Fe}_3\text{SO}_4$  with magnetic properties has started receiving attention by researchers [14]. Co-doping of ZnO can influence the performance of this photocatalysts. This affects the dynamics of electron hole pair recombination and interfacial charge transfer. The largest enhancement of photoactivity through doping can be found in nano sized particles [14]. Selenium is a trace element, very essential for normal health and reproduction. It was considered as a poison until it was identified as a micronutrient for bacteria, mammals and

birds. Selenium is essential for the effective operation of the immune system in both animals and humans. It has received considerable attention because of its remarkable biological applications such as anticancer, antimicrobial, antidiabetic and antioxidant activities [17, 5]. Research is under progress to extract the medicinal applications of selenium nanoparticles such as anticancer [6], antimicrobial [13], orthopaedic or malignant mesothelioma [7]. Results from epidemiological, ecological clinical studies have shown selenium decreases the risk of some cancers such as prostate, lung and colon cancer. Selenium nanoparticles are also known for their remarkable applications such as photodegradation, photoconductivity and wastewater treatment.

Exfoliated graphite (EG) is an excellent inorganic carbon material with a porous structure, which has many characteristics including low density, non-toxicity, non-pollution and easy disposal. Because of its porous structure, this material has been used as an absorbent for removing organic pollutants from wastewater, such as oils, biomedical liquids and dyes [9, 17].

## EXPERIMENTAL

### Materials

Natural graphite (NG) flakes, zinc chloride, selenium metal and sodium selenite were purchased from Sigma Aldrich while sulphuric acid, nitric acid, polyethylene glycol, ammonia and methylene blue dye were obtained from Merck Chemicals. All chemicals and reagents were purchased from credible suppliers and used without further purification. The purity of such chemicals was ascertained to be acceptable for the intended reactions. Deionized water was used for all calibration and solution preparations.

### Synthesis of Exfoliated Graphite

Natural graphite was soaked in  $\text{H}_2\text{SO}_4$ :  $\text{HNO}_3$  (3:1v/v) acid mixture overnight and washed several times with deionized water until the water had no sulphate ion and pH was neutral. The product, graphite intercalated compound (GIC), was dried in an oven ( $100^\circ\text{C}$ ). The GIC was subjected to thermal treatment in an electric furnace at  $800^\circ\text{C}$  for about 1 min forcing the intercalated material out of the graphite lattice, thereby rupturing the layers. This procedure resulted in the puffed material called exfoliated graphite that is characterized by a very low density of 0.0068 g/ml.

#### *Synthesis of EG/Se-ZnO Nanocomposites*

Zinc chloride (1.36 g) was added to 200 ml of deionized water in a beaker and stirred. Exfoliated graphite (20 mg) and Selenium (16 mg) metal were then added and the mixture was left to stir for hours. Polyethylene glycol (4 ml) and aqueous ammonia (4 ml) were gradually added while stirring and this was left to stir for several hours. The mixture was washed with both deionized water and ethanol during filtration and dried in an oven for 2 hours at a temperature of 80°C. The nanocomposite was obtained after calcinations at 400°C for 3 hours.

#### *Characterization*

X-ray diffraction (XRD) measurements were performed using Rigaku Ultima IV diffractometer operated at 40 kV and 40 mA. The Cu K $\alpha$  radiation ( $\lambda=0.15406$  nm) as the source. FT-IR spectra were obtained on a Perkin Elmer Spectrum 100 FT-IR spectrometer at a resolution of 4 cm<sup>-1</sup>, averaging 30 scans. Scanning electron microscopy (SEM) images were obtained on a Vega 3 XMU instrument and transmission electron microscopy (TEM) analysis was performed on JEOL (JEM-2100 electron microscope).

#### *Photocatalytic degradation*

The photocatalytic activities of synthesized EG/Se-ZnO were quantified by measuring the rate of degradation of methylene blue under simulated solar irradiation. Nanocomposite material (0.1 g) was suspended in 100 ml of methylene blue solution of concentration 20 ppm. A solar simulator (Oriel, Newport), with an Oriel Xenon lamp (500 W) was employed as a radiation source. The power output was set to 300 W in order to give irradiance of 1000 Wm<sup>-2</sup> at 25°C, without the cover glass and preferably emitting UV radiation. An Oriel PV reference cell system equipped with a 2 cm $\times$ 2 cm monocrystalline silicon photovoltaic cell and a Type K thermocouple was used to set the simulator irradiance. Prior to photocatalytic reactions, the suspensions were magnetically stirred in the dark for 30 minutes to allow for adsorption equilibrium before UV light illumination. Aliquots of the suspension (4 ml) were withdrawn at constant time intervals using a 10 ml Neomedic disposable syringe and filtered through a 0.22  $\mu$ m PVDF membrane filter for various periods of irradiation up to 180 mins. Variations in the concentrations of the dye were monitored on a UV-Vis spectrophotometer (Cary 60 UV-vis, Agilent Technologies) at  $\lambda=615$  nm.

#### *Determination of antibacterial activity (Agar well diffusion method)*

Antibacterial activity of nanocomposite was evaluated by the agar well diffusion method using modified [1]. The microbial cultures were adjusted to equal 0.5 McFarland turbidity standards and inoculated on Mueller Hinton agar (MHA, oxid) plate (diameter 9 cm) by flooding the plate with 1ml of each of the standardized test organism, swirled and excess inoculum was carefully decanted. A sterile cork borer was used to make wells (6 mm in diameter) on the agar plates. Aliquots of 0.1ml of nanoparticle dilutions, reconstituted in 50% DMSO at concentrations of 5 mg/ml and 2.5 mg/ml were applied on each of the well in the culture plates previously inoculated with the test organisms. However, each extract was tested in triplicate with 0.1ml and 5 $\mu$ g/ml of ciprofloxacin as positive control. These were left on the bench for 1 hour for proper diffusion of the nanoparticles [12].

Thereafter, the plates were incubated at 37°C for 24 hours without inversion. Antibacterial activity was determined by measuring the zone of inhibition around each well (Excluding the diameter of the well) for each nanoparticle, triplicate test were conducted against each organism.

## **RESULT AND DISCUSSION**

#### *Characterisation*

The synthesis of ZnO and EG/Se-ZnO were followed by characterization using XRD, FTIR, SEM, EDS and TEM. From the XRD result shown in fig. 1a below the peak observed at 26.7° is characteristics of interlayer stacking of aromatic systems indexed as a (0 0 2) peak of Exfoliated Graphite. Different peaks at 31.9, 34.5, 36.4, 47.7, 56.7, 62.9, 66.5, 68.1 and 69.2 which match to the (1 0 0), (0 0 2), (1 0 1), (1 0 2), (1 1 0), (1 0 3), (2 0 0), (1 1 2) and (2 0 1) crystalline plane of ZnO respectively. This data confirmed the hexagonal wurtzite structure of ZnO (JCPDS No. 36-1451). Also peaks at 72.65 and 77.13 indicate the presence of Selenium.

The formation of composite photo-catalyst was also confirmed by FT-IR spectra (Fig. 1b). A sharp peak around 1650 cm<sup>-1</sup> indicates H—O—H bending vibration, which is allocated to a small amount of H<sub>2</sub>O in the ZnO crystal. Another band at 882 cm<sup>-1</sup> is associated to the vibrational frequency of ZnO lattice. The appearance of the peak around 612, 727 and 1373 cm<sup>-1</sup> confirms the presence of Selenium and all these confirmed the nanocomposites.

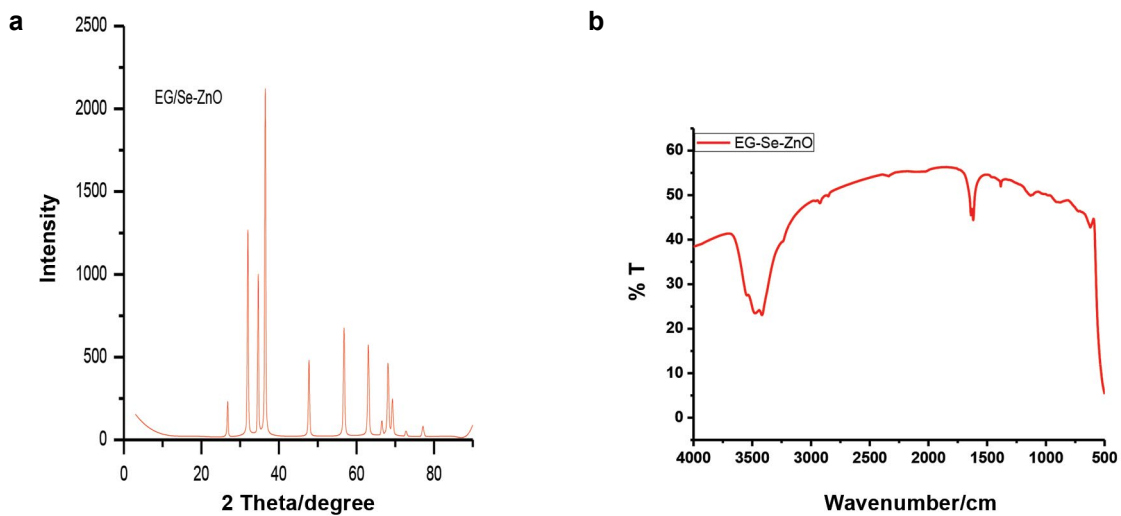


Fig. 1. (a) XRD and (b) FTIR spectra of EG/Se-ZnO.

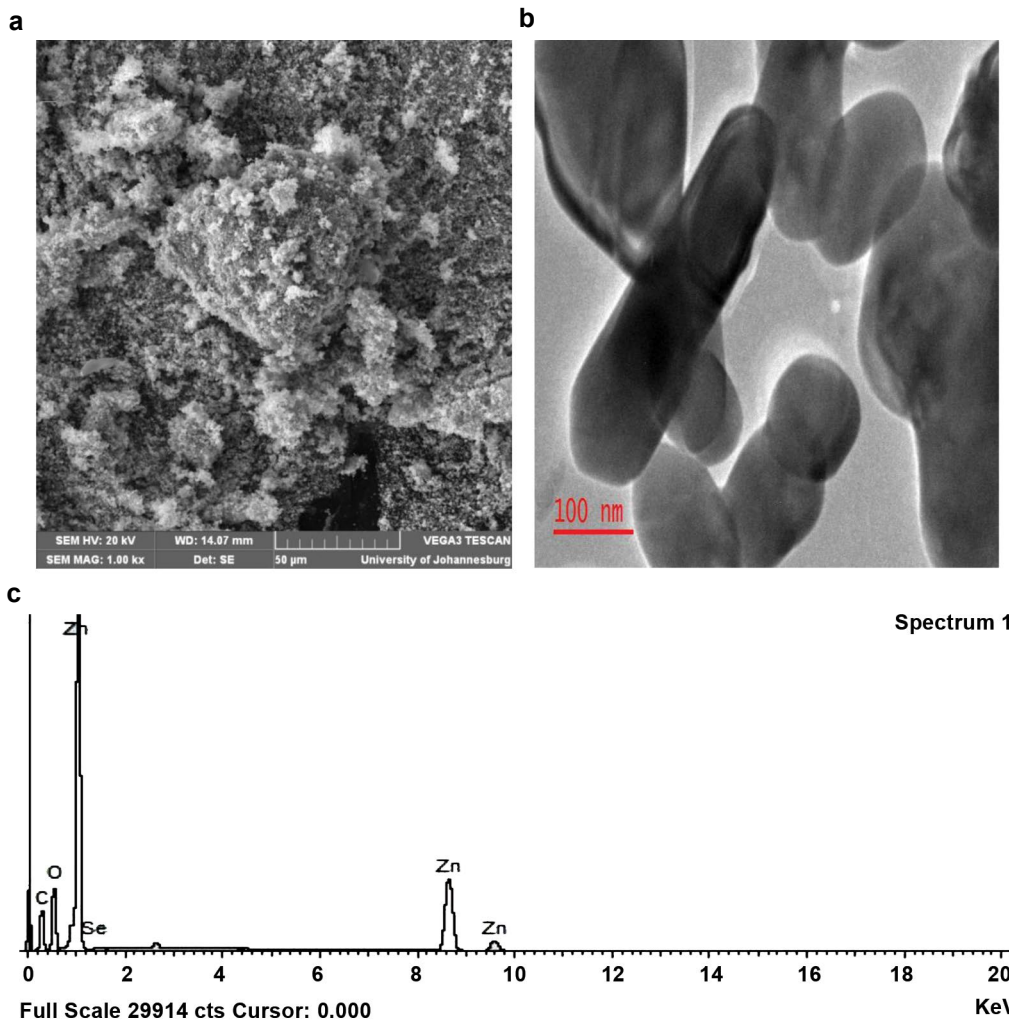


Fig. 2. (a) SEM image, (b) TEM image and (c) EDS spectra of EG/Se- ZnO nanocomposite.

The SEM image (fig. 2a) showed the EG/Se-ZnO composite with cloudy large nanoclusters with agglomerated particle. It was difficult to estimate the actual size of single particles due to aggregation. Figure 2b showed the TEM image of EG/Se-ZnO nanocomposite with a nano-rod structure. The elemental composition of the composite was estimated by EDS. EDS spectra of the co-doped ZnO (fig.2c) showed signal directly related to the dopants. Results confirmed the presence of Zn, O, Se and C (EG) indicating the formation of EG/Se-ZnO composite. The low dopant amount of EG and Se resulted in corresponding weak EDS peaks.

*Photodegradation of methylene blue*

In the EG/Se-ZnO composite, the degradation efficiency of ZnO was the primary cause of the dye removal, while the main function of EG was

to make the dye absorbed onto the composites and provide deposition site as well as growth of hydrolysis products. Due to the characteristic pore structure of EG, a large amount of Uv light could penetrate through the pores and irradiate. EG has an exceptionally good electron channeling property because of its extensive  $\pi$  electron system. Formation of bond between the composites (EG/Se-ZnO) promotes electron transfer with EG acting as electron trapping site. This enhances the lifetime of holes which participates in pollutant oxidative degradation. A dye removal efficiency of 99.5% under Uv light irradiation at 90 mins was observed for the EG/Se-ZnO nanocomposite as shown in Fig. 3a.

The photodegradation of methylene blue obeyed the Langmuir-Hinshelwood first order kinetics;

$$\ln(C_0/C) = k(t)$$

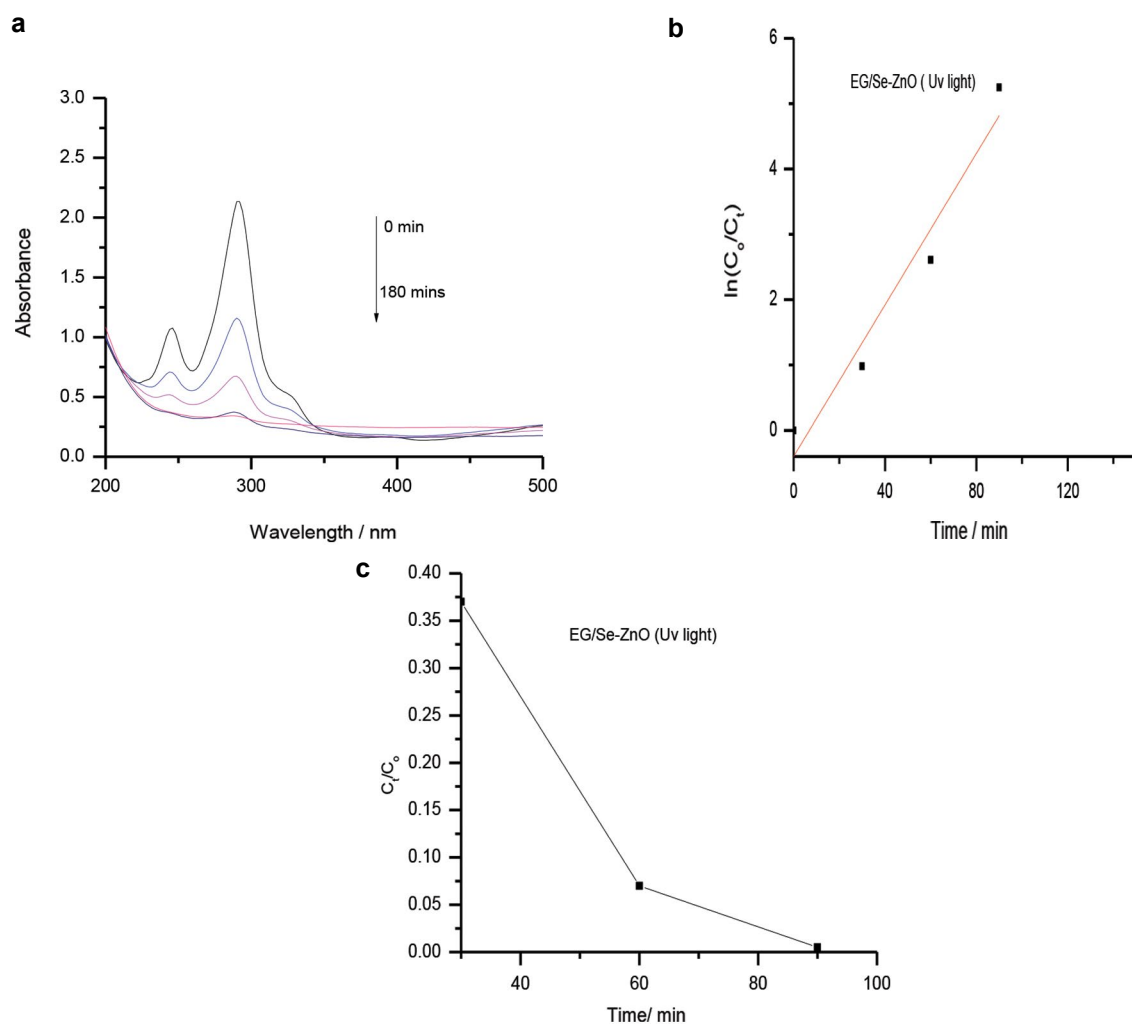


Fig. 3. (a) Methylene blue degradation profile, (b) Kinetics of methylene blue degradation and (c) Normalized photodegradation trend.



Where  $C_0$  is the initial methylene blue concentration,  $C$  is the concentration of the dye at time  $t$  and  $k$  is the rate constant [16]. Good linear fits were observed for EG/Se-ZnO indicating that the reaction followed first order kinetics. The rate constant and  $R^2$  value for EG/Se-ZnO was  $5.79 \times 10^{-2} \text{ min}^{-1}$  and 0.9 respectively. It has also been demonstrated that introducing reduced graphene oxide into a semiconductor nanoparticle matrix boosts its photocatalytic and photo electrochemical performance [17]. Since EG is composed of a larger number of graphene sheets, the same behavior may be expected. However, the mechanism behind such enhanced performance has not been fully explored [4].

The antibacterial activity of ZnO (Bulk) and

EG/Se-ZnO nanocomposite were evaluated by agar well diffusion method. The study evaluated the ability of this nanocomposite as antibacterial agent against two gram-negative bacterial strains which are water borne pathogens. The antibacterial activity was determined by measuring the zone of inhibition in nm (Table 1). The highest inhibition was observed with EG/Se-ZnO for the growth of the bacterial strains at concentration 5.0 mg, while ZnO (bulk) records the moderate zone of inhibition against tested organisms; *E.coli* and *E. cloacae*. The histogram in figure 4 conspicuously showed that the inhibition of the composite (EG/Se-ZnO at 5.0) on both bacteria is higher than ZnO only at 2.5 and appreciably closer to the standard, ciprofloxacin.

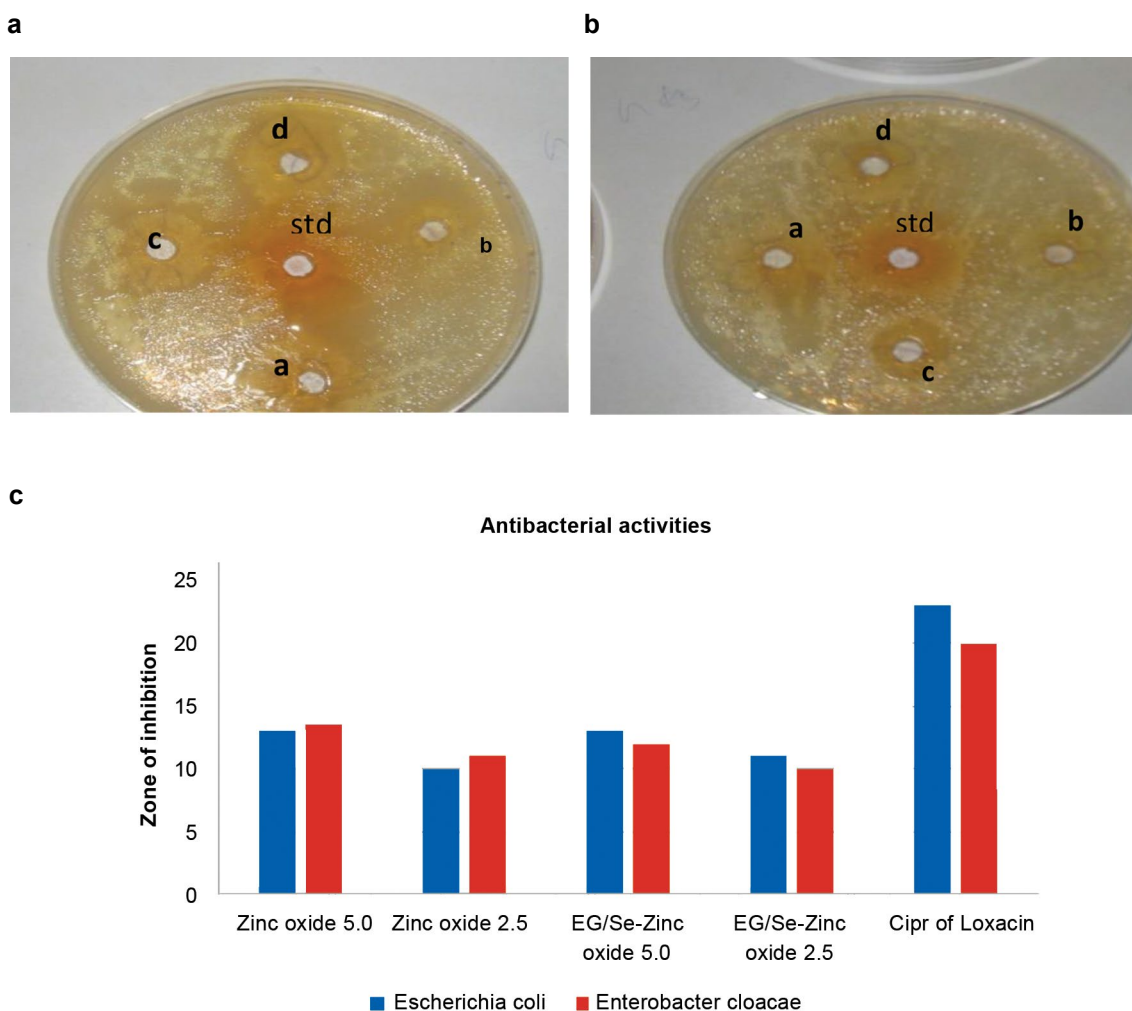


Fig. 4: Plate 1 is showing the antibacterial activity of nanoparticles ; (a) Zinc oxide (Bulk) 5.0 mg, (b) Zinc oxide (Bulk) 2.5 mg, (c) EG/Se-ZnO 5.0 mg and (d) EG/Se-ZnO 2.5 mg against Escherichia coli and Plate 2 showing the antibacterial activity of nanoparticles; (a) Zinc oxide (Bulk) 5.0 mg, (b) Zinc oxide (Bulk) 2.5 mg, (c) EG/Se-ZnO 5.0 mg and (d) EG/Se-ZnO 2.5 mg against Enterobacter cloacae. (3) Histogram is showing the comparison of the antibacterial activities of the composites.

Table 1: Showing the antibacterial activities of Zinc oxide and EG/Se-Zinc oxide

Nanoparticles/ Concentration(mg)	<i>Escherichia coli</i>	<i>Enterobacter cloacae</i>
Zinc oxide 5.0	13	14
Zinc oxide 2.5	10	11
EG/Se-Zinc oxide 5.0	13	12
EG/Se-Zinc oxide 2.5	11	10
Ciprofloxacin	23	20

## CONCLUSION

Nanocomposite EG/Se-ZnO photocatalyst powders were synthesized by reduction process and eco-friendly method. It was then characterized using XRD, FTIR, SEM and TEM. The highest peak of XRD spectra was observed at 101 and comparison to solvent is invariant (002), i.e. diffusion ion was free from solvent viscosity. FTIR confirmed the formation of EG/Se-ZnO composite as band at  $882\text{ cm}^{-1}$  and  $612\text{ cm}^{-1}$ ,  $727\text{ cm}^{-1}$ ,  $1373\text{ cm}^{-1}$  were associated with vibrational frequency of ZnO lattice Selenium respectively. SEM revealed cloudy large particles of the synthesized EG/Se-ZnO composite as agglomerated particle with estimation of size of single particle was difficult. The nano-rodlike structure of EG/Se-ZnO was revealed with TEM. Photodegradation by this semiconductor photocatalyst offers a green technology for the removal of hazardous compounds present in the industrial effluents. Antibacterial activity of the nanocomposite synthesized was tested against two gram-negative bacteria with the zone of inhibition observed on *Escherichia coli* and *Enterobacter cloacae* were 14 mm and 12 mm respectively in comparison while the bulk ZnO had 13 mm zone of inhibition. EG/Se-ZnO nanocomposite is a promising material that could serve as a dual-purpose agent: antibacterial and photocatalyst degradation agent of dye.

## ACKNOWLEDGMENT

The authors would like to thank the Centre for

Nanomaterials Science Research, Department of Applied Chemistry and University of Johannesburg, South Africa.

## CONFLICT OF INTEREST

The authors declare that there is no conflict of interests regarding the publication of this manuscript.

## REFERENCES

- P. Aida, V. F. Rosa Blamea, A. Thomas and C. Salvador. J. Ethnopharmacol. Short Comm. 16 (2001) 93-98.
- A. A. Abdullah. Journal of Biomaterials and Nanobiotechnology. 8 (2017) 66-82.
- B. Abebe, P.Y. Om and D. Tania. Environ Sci Pollut Res 6 (2016), 7750-6
- N.J. Bell, Y.H. Ng, A. Du, H. Coster, S.C. Smith and R. Amal. J. Phys. Chem. C, 115 (2011) 6004-6009.
- L.C. Clark, G. F. Combs, B. W. Turnbull, E. H. Slate, D. K. Chalker, J. Chow, J. R. Taylor. J. Am Medical Ass, 276 (1996) 1957-1963.
- N. Helin, W. Qinmin, L. Hongxia, C. Min, M. Changjie, S. Jiming, Z. Shengyi, G. Yuanhao and C. Changle. Materials 7 (2014) 4034-4044.
- P. V. Lakshmi and R. Vijayaraghavan. Scientific Reports 6 (2016) 38606.
- S. D Lambert, N. J. D. Graham, C. J. Sollars and D. D. Fowler. Water Sci. Technol. 36 (2-3) (1997) 173.
- J.T. Li, M. Li, J. H. Li and H.W. Sun. Handbook on Applications of Ultrasound: Sonochemistry for Sustainability. Ultrason. Sonochem. (Vol. 14) (2007).
- O. A. Mohd, M. K. Mohammad, A. A. Sajid, H. C. Moo. Journal of Saudi Chemical Society 19 (2015) 494-50.
- R. P. Manohar and V. S. Shrivastava. Chemica Sinica 5 (2014) 8-17.
- National Committee for Clinical Laboratory Standards (NCCLS), (1990). Man. Clin. Microbiol., 5th Ed.
- A. T. Phong, and J. W. Thomas. 6 (2011) 1553-1558.
- K.B. Purna, B. Priyakshree, D. Gitashree, K. K. Chaitanya, K. Indrapal, V.S. Manjusha, P. Pallabi, S. Dulen and R. D. Manash R. D. RSC Adv. 6 (2016) 11049
- M. Sangareswari and M. M. Sundaram. IRJET 2 (2015) 526-537.
- M. Savoskin, A. Yaroshenko, N. Lazareva, V. Mochalin, and R. Mysyk. J. Phys. Chem. Solids, 67 (2006) 1205-1207.
- N. Thabile, T. K. Alex, A.O. Arotiba, S. Srinivasan, W. K. Rui and B.M. Bhekie. Applied Surface Science 300 (2014) 159-164.
- H. Wang and C. S. Xie, J. Phys. Chem. Solids (Nanomaterial) 69 (2008).